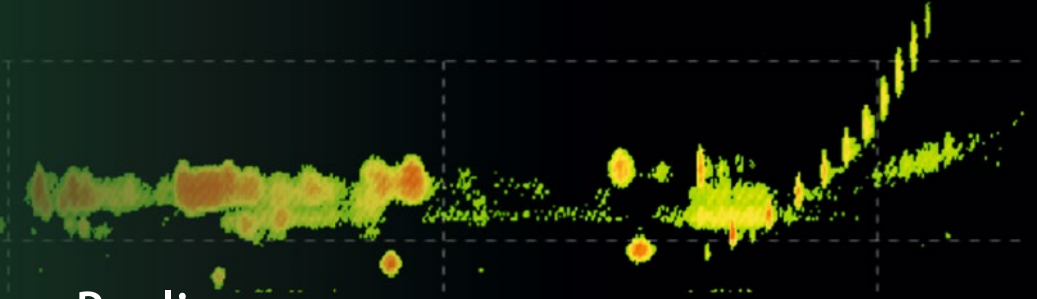


Methods in  
Molecular Biology 2084

Springer Protocols



Giuseppe Paglia  
Giuseppe Astarita *Editors*

# Ion Mobility–Mass Spectrometry

Methods and Protocols

 Humana Press

# METHODS IN MOLECULAR BIOLOGY

*Series Editor*

**John M. Walker**

**School of Life and Medical Sciences**

**University of Hertfordshire**

**Hatfield, Hertfordshire, UK**

For further volumes:

<http://www.springer.com/series/7651>

For over 35 years, biological scientists have come to rely on the research protocols and methodologies in the critically acclaimed *Methods in Molecular Biology* series. The series was the first to introduce the step-by-step protocols approach that has become the standard in all biomedical protocol publishing. Each protocol is provided in readily-reproducible step-by-step fashion, opening with an introductory overview, a list of the materials and reagents needed to complete the experiment, and followed by a detailed procedure that is supported with a helpful notes section offering tips and tricks of the trade as well as troubleshooting advice. These hallmark features were introduced by series editor Dr. John Walker and constitute the key ingredient in each and every volume of the *Methods in Molecular Biology* series. Tested and trusted, comprehensive and reliable, all protocols from the series are indexed in PubMed.

# **Ion Mobility-Mass Spectrometry**

## **Methods and Protocols**

Edited by

**Giuseppe Paglia**

*Department of Medicine and Surgery, University of Milano-Bicocca, Vedano al Lambro,  
Monza e Brianza, Italy*

**Giuseppe Astarita**

*Georgetown University, Washington, DC, USA*

 **Humana Press**

*Editors*

Giuseppe Paglia  
Department of Medicine and Surgery  
University of Milano-Bicocca  
Vedano al Lambro  
Monza e Brianza, Italy

Giuseppe Astarita  
Georgetown University  
Washington, DC, USA

ISSN 1064-3745

ISSN 1940-6029 (electronic)

Methods in Molecular Biology

ISBN 978-1-0716-0029-0

ISBN 978-1-0716-0030-6 (eBook)

<https://doi.org/10.1007/978-1-0716-0030-6>

© Springer Science+Business Media, LLC, part of Springer Nature 2020

This work is subject to copyright. All rights are reserved by the Publisher, whether the whole or part of the material is concerned, specifically the rights of translation, reprinting, reuse of illustrations, recitation, broadcasting, reproduction on microfilms or in any other physical way, and transmission or information storage and retrieval, electronic adaptation, computer software, or by similar or dissimilar methodology now known or hereafter developed.

The use of general descriptive names, registered names, trademarks, service marks, etc. in this publication does not imply, even in the absence of a specific statement, that such names are exempt from the relevant protective laws and regulations and therefore free for general use.

The publisher, the authors, and the editors are safe to assume that the advice and information in this book are believed to be true and accurate at the date of publication. Neither the publisher nor the authors or the editors give a warranty, express or implied, with respect to the material contained herein or for any errors or omissions that may have been made. The publisher remains neutral with regard to jurisdictional claims in published maps and institutional affiliations.

This Humana imprint is published by the registered company Springer Science+Business Media, LLC, part of Springer Nature.

The registered company address is: 233 Spring Street, New York, NY 10013, U.S.A.



## Metabolomic Profiling of Adherent Mammalian Cells In Situ by LAESI-MS with Ion Mobility Separation

Sylwia A. Stopka and Akos Vertes

### Abstract

Ambient ionization-based mass spectrometry (MS) methods coupled with ion mobility separation (IMS) have emerged as promising approaches for high-throughput in situ analysis for biomedical to environmental applications. These methods are capable of direct profiling and molecular imaging of metabolites, lipids, peptides, and xenobiotics from biological tissues with minimal sample preparation. Furthermore, employing IMS within the workflow improves the molecular coverage, resolves isobaric species, and improves biomolecule identifications through accurate collision cross section measurements. Laser ablation electrospray ionization (LAESI)-MS coupled with IMS has been successful in profiling and molecular imaging of small biomolecules directly from biological tissues and single cells. Herein, we describe a protocol for the direct analysis of adherent mammalian cells with limited perturbations by LAESI-IMS-MS. A benefit of IMS is that within the same LAESI acquisition, the spectral features related to the ESI background, washing buffer, and cell signal can be extracted and isolated separately.

**Key words** Mass spectrometry, Ion mobility separation, Cell culture, Metabolites, In situ analysis, Laser ablation electrospray ionization, LAESI-IMS-MS

---

## 1 Introduction

To uncover the relationship between the genotype and phenotype of a biological system, a comprehensive analysis that encompasses genomics, transcriptomics, proteomics, and metabolomics is needed. Of these omics, metabolomics is the least established due to a variety of challenges, e.g., the wide range of metabolite concentrations, varied compound polarities, and the diverse classes of compounds [1]. Due to their high sensitivity and selectivity, mass spectrometry (MS)-based platforms have been at the forefront in the detection, identification, quantification, and spatiotemporal mapping of biomolecules. The most common MS workflow for metabolite analysis and quantification includes liquid chromatography (LC) combined with stable isotope labeling. For example, the absolute metabolite concentrations (ranging from millimolar to

nanomolar) and fluxes of over 150 compounds were determined for immortalized baby mouse kidney cells (IBMK) [2]. However, this analysis requires extensive sample preparation, is considered low-throughput, and does not capture any spatial information of biomolecules within the tissue.

Ambient ionization MS methods provide an alternative approach for metabolite, lipid, peptide, and xenobiotic analysis and imaging from biological tissues with minimal sample preparation and under native conditions. A large number of ambient sampling methods have been introduced including liquid-based, plasma-based, and laser-based approaches [4, 5]. Due to the wide versatility and adaptability of these techniques, applications in biomedical research have covered microbe-host interactions, environmental studies, molecular imaging, and forensics problems [6–9]. Among these, the more established methods include desorption electrospray ionization (DESI), direct analysis in real time (DART), and laser ablation electrospray ionization (LAESI) [10–12]. Due to the high water content found in biological tissues and cells, laser-based approaches that operate in the mid-IR range have been a useful tool for in situ analysis. Here a mid-IR laser beam tuned to the strongest absorbance maximum of water (2940 nm), which corresponds to the symmetric stretching of the O–H bonds, is focused onto the sample resulting in an ablation plume that is ionized by electrospray ionization (ESI). To afford high-throughput and direct sampling capabilities, ambient ionization methods typically omit separation methods, e.g., HPLC, which results in spectral complexity and ion suppression effects.

To retain the benefits of a separation step in combination with direct sampling, ion mobility separation (IMS) can be introduced. This expands the molecular coverage, improves the signal-to-noise ratio, increases confidence in molecular identification through determining the ion collision cross section (CCS), and resolves isobaric species [13–16]. In this gas phase separation, ions are differentiated within milliseconds based on their size, shape, and charge state [17, 18]. The benefits are clearly observed when coupling LAESI-MS with IMS, which have been demonstrated for high-throughput metabolite profiling of living algal cells and plant tissues, identification of isotopologues, determination of turnover rates for small molecules, and separation of compound classes [19, 20].

As many new therapies and diagnostic tools for human disease are based on cellular models, the ability for in situ analysis of adherent mammalian cells is valuable in biology and medicine [21, 22]. To minimize cell manipulation, e.g., lysis and enzymatic digestion that may affect the physiological state and alter biochemical processes, direct sampling is beneficial [23]. Herein, we outline a protocol using LAESI-MS coupled with IMS for the direct

analysis of adherent mammalian cells. Separation and isolation of ions related to the ESI background, washing buffer, and cells with limited sample preparation is demonstrated with IMS.

---

## 2 Materials

### 2.1 Reagents and Chemicals

1. Electrospray solution for negative ion mode: methanol:chloroform (2:1, v/v).
2. Dulbecco's Modified Eagle's Medium (DMEM) (ATCC 30-2002) supplemented with 10% fetal bovine serum (FBS) (ATCC 30-2020), 1% MEM nonessential amino acid solution (100 $\times$ ), and 1% penicillin–streptomycin for cell culture.
3. Phosphate-buffered saline (PBS) (ThermoFisher, Waltham, MA) for cell washing and 0.25 $\times$  trypsin-EDTA for cell detachment.
4. 70% ethanol for sterilization.

### 2.2 Biological Samples and Materials

1. Cryogenic stock of human neuroblast (SK-N-AS; ATCC CRL-2137) derived from brain and bone marrow (*see Note 1*).
2. Humidity-controlled cell incubator set at 5% CO<sub>2</sub> and 37 °C.
3. Automated cell counter.
4. Ethanol-sterilized microscope slides.
5. 100 cm polystyrene petri dish.

### 2.3 LAESI-IMS-MS

#### 2.3.1 Electrospray

1. The electrospray assembly consists of a conductive union, an insulating mounting bracket, fused silica tubing, a needle port (IDEX Health and Science, Oak Harbor, WA), and a 50  $\mu$ m ID-tapered metal emitter (MT320-50-5-5; New Objective, Woburn, MA). The ESI assembly is mounted on a three-axis translation stage using optical posts. The ESI emitter tip should be positioned on axis and 12 mm from the mass spectrometer orifice.
2. High voltage (–2.7 kV) is applied to the conductive union by a regulated power supply (PS350; Stanford Research Systems, Sunnyvale, CA) through a high-voltage cable (*see Note 2*).
3. A syringe pump is used to supply the ESI solution at a 500 nL/min flowrate from a 500  $\mu$ L syringe.

#### 2.3.2 Laser Ablation

1. A mid-IR laser source (Opolette 100; Oportek, Carlsbad, CA) used is tuned to 2940 nm wavelength for maximum absorbance. The produced laser pulses are 5 ns in length and are emitted at a repetition rate of 20 Hz. The laser beam is steered with gold-coated mirrors through a 30 mm cage system from the laser cavity to the last optical component (*see Note 3*).



2. A 75 mm planoconvex focal length ZnSe lens (Infrared Optical Products, Farmingdale, NY) is used to focus the mid-IR laser beam on the sample. The microscope slide containing the adherent cells is mounted on an XYZ stage that is positioned 15 mm below the orifice–ESI axis. The alignment diode can be used to visualize the laser beam on the sample surface.
3. Assure that the laser beam is focused by firing single shots at thermal paper and use a microscope to observe the produced spot size. Adjust the distance between the lens, and the sample until the spot is circular and shows minimum size.

### 2.3.3 IMS Configuration

1. A homebuilt LAESI source is retrofitted to the front end of a commercial quadrupole time-of-flight mass spectrometer (Synapt G2S; Waters, Milford, MA). This system is equipped with a traveling-wave (T-wave) IMS with a resolving power of  $\Omega/\Delta\Omega = 30$ .
2. Nitrogen is used as the drift gas and supplied at a flow rate of 90 mL/min, a pressure of 3.35 mbar, and a delay coefficient of 1.41 V (*see Note 4*).
3. The height and velocity of the traveling wave were set to 40 V and 650 m/s, respectively.
4. Ion collision cross section (CCS) values were derived using polyalanine oligomers with  $n = 3$ –14 as the calibrant. This calibration method covered the  $m/z$  range from 230 to 1011.

---

## 3 Methods

### 3.1 Sample Preparation

1. Using a glass pen scribe, cut to three parts of similar dimension  $75 \times 25 \text{ mm}^2$  microscope slides. Sterilize them with 70% ethanol and UV light on both sides in a sterile environment. Arrange the cut slides next to each other in a 100 cm petri dish covering most of the dish without any overlap. Smaller microscope slides afford shorter measurement times thereby improve reproducibility.
2. Culture the stock SK-N-AS cells in the supplemented DMEM medium in a T75-uncoated culture flask. The medium is aspirated from the flask, washed once with  $1 \times$  PBS, and filled with 4 mL of prewarmed trypsin (*see Note 5*).
3. Place the flask in the incubator for 10 min to allow the cells to detach from the surface. Add prewarmed fresh DMEM medium to the flask to inactivate the trypsin.
4. Use a cell counter to determine the cell density and then dilute to  $5 \times 10^5$  cells/mL. This cell suspension is then pipetted (500  $\mu\text{L}$ ) onto the sterilized cut microscope slides. Place the petri dish in the incubator for  $\sim 15$  min, so the cells can adhere

to the slides. Prewarmed fresh medium is gently poured into the petri dish without disturbing the slides until the dish is  $\frac{3}{4}$  filled. Place back the petri dish into the incubator and perform LAESI analysis 1 h later.

### 3.2 LAESI Direct Analysis of Adherent Mammalian Cells

1. Assemble both the ESI and LAESI optical components as mentioned in Subheading 2. Run the ESI for 30 min to assure a stable spray prior to any analysis.
2. Place the mass spectrometer into operational mode and perform the appropriate mass and drift time (DT) calibrations using sodium formate and polyalanine, respectively. LAESI mass spectra should be obtained for both calibration events.
3. Once the LAESI source is optimized, the slides containing the SK-N-AS cells can be analyzed. A slide is removed from the medium with tweezers, gently rinsed with  $10\times$  diluted PBS, and placed onto the sample mount for analysis.
4. Start the data acquisition, the first ten scans are of the ESI background followed by firing the laser and rastering the laser beam over the cell surface. Sample related ions can be tracked using their ion chromatogram.
5. End the acquisition by stopping the laser from firing, turning off the ESI high-voltage power supply and the syringe pump. Place the instrument in standby mode.
6. The acquired data are ready to be processed.

### 3.3 Separation and Classification of Small Molecules from LAESI Data

1. Using the IMS feature, the data sets can be visualized as a DT vs.  $m/z$  plot showing the ion intensities on a false color scale using the DriftScope 2.4 software (Waters, Milford, MA). Here the sample-related peaks, PBS ion clusters, and ESI background ions can be differentiated as red, teal, and blue dots, respectively (*see* Fig. 1a). Regions of interest can be extracted individually to produce enhanced mass spectra with reduced spectral interferences for the three different groups (*see* Fig. 1b–d).
2. As each ion appears at a specific DT range based on its size, shape, and charge state, looking at the DT distributions results in separation and improved signal-to-noise ratios. From the LAESI mass spectrum of the SK-N-AS cells, several metabolites can be identified using tandem MS, database searches and the CCS measurements on the order of milliseconds (*see* Fig. 2). Small molecules, e.g., adenine and glutamine have shorter DT values compared to lipids.
3. The CCS calibration is applied after data acquisition using the DriftScope 2.4 software and correlates the polyalanine unit drift times with the CCS values (Table 1). For our example, the related equation is  $\Omega_{\text{calibration}} = A(t'_d)^B$ , in which

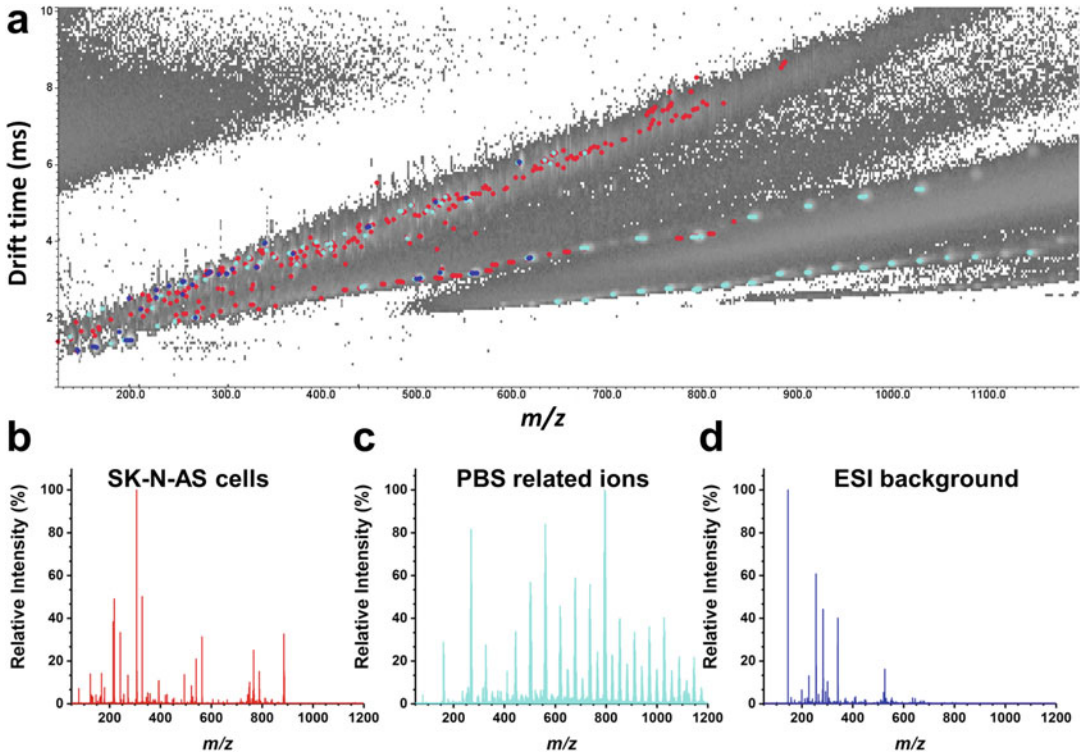


**Fig. 1** (a) A DT vs.  $m/z$  map corresponding to a LAESI mass spectrum of adherent SK-N-AS neuroblasts in  $10\times$  diluted PBS. Separation of ions related to the cells, PBS, and ESI background within the plot is displayed in red, teal, and blue dots, respectively. To enhance the ion signal and provide spectral separation for each group, three selected regions within the DT vs.  $m/z$  plot were extracted into individual mass spectra containing the (b) cells, (c)  $10\times$  diluted PBS, and (d) ESI-related ions

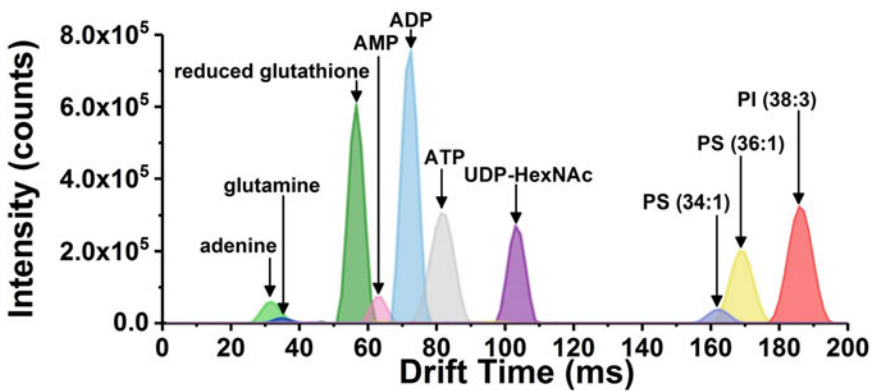


**Fig. 2** Measured DT distributions for several metabolites and lipid species from a typical LAESI mass spectrum of SK-N-AS neuroblasts

**Table 1**  
**Measured CCS<sub>nitrogen</sub> and DT values for polyaniline oligomers with  $n = 3-14$  in negative ion mode**

$n$	$m/z$	DT (ms)	CCS (N <sub>2</sub> ) (Å <sup>2</sup> )
3	230.117	35	150
4	301.159	41	165
5	372.199	48	179
6	443.237	57	195
7	514.274	65	209
8	585.312	72	223
9	656.348	80	238
10	727.392	89	253
11	798.427	98	267
12	869.471	107	279
13	940.512	117	294
14	1011.547	127	308

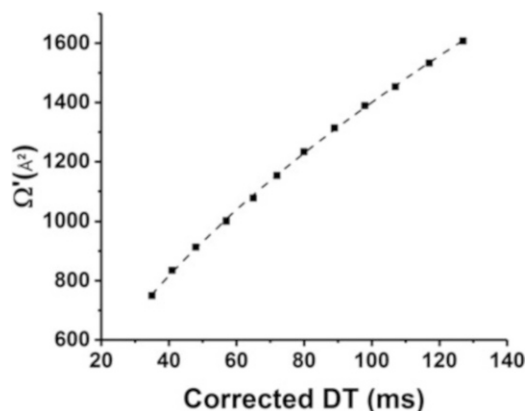


**Fig. 3** Polyaniline CCS calibration plot for  $n = 3-14$  oligomers using nitrogen buffer gas in negative ion mode. The corrected DT reflects mass-independent flight times

$A = 466.443$ , and  $B = 0.573$ , and  $R^2$  is 0.9996 (see Fig. 3). This calibration is then applied to the LAESI DT vs.  $m/z$  plots that correlate the detected ion  $m/z$  values with the CCS.

4. Extract all CCS measurements and  $m/z$  values using the Drift-Scope 2.4 software.
5. Plotting CCS vs.  $m/z$ , some classes of homologous compounds can be revealed based on observed trends, e.g., amino

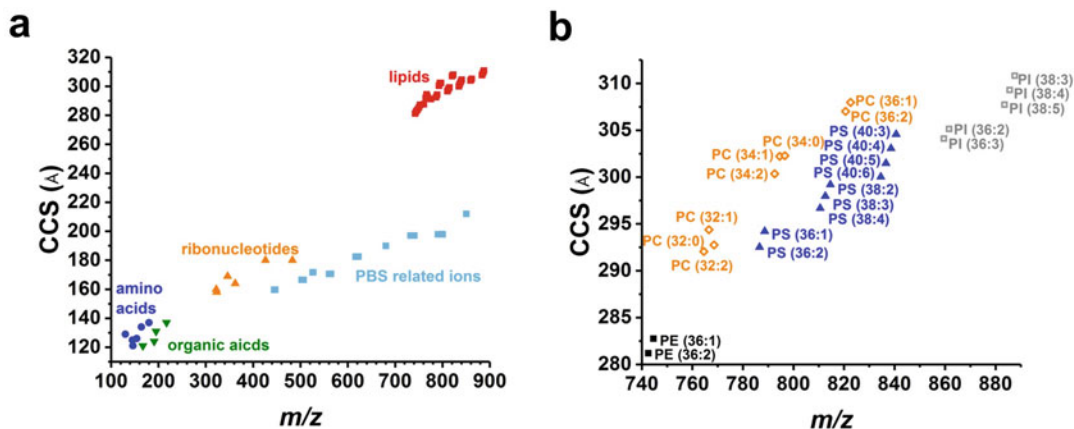


**Fig. 4** (a) A CCS vs.  $m/z$  plot that reveals separation and classification of detected metabolites from adherent SK-N-AS cells analyzed by LAESI-IMS-MS. Unique trends were observed for each homologous class of molecules and the PBS-related ions. (b) A zoomed area within the lipid region from the CCS vs.  $m/z$  plot revealed separation of specific lipid classes as well as trends based on degree of saturation. The lipid species phosphatidylethanolamine (PE), phosphatidylserine (PS), and phosphatidylinositol (PI) were detected as  $[M-H]^-$  species, whereas the phosphatidylcholine (PC) species were detected as  $[M+Cl]^-$  adducts

acid CCS values were within 121–137 Å<sup>2</sup>, ribonucleotides ranged between 158 and 180 Å<sup>2</sup>, and lipids within 281–310 Å<sup>2</sup> (see Fig. 4a).

- Examining the lipid species in the CCS vs.  $m/z$  plot, revealed separation based on lipid class and degree of saturation (see Fig. 4b). For example, the phosphatidylethanolamine lipids have smaller headgroups than phosphatidylserines and phosphatidylinositols, thus they have a smaller CCS values than the two latter lipid classes.

## 4 Notes

- The SK-N-AS cells are biosafety level one (BSL-1), thus all cell handling should be performed in a BLS-1-rated hood. Personnel working with these cells should undergo biohazard training. Additionally biohazard signs should be placed on all equipment and instruments that may come in contact with the cells.
- Extreme caution should be used when dealing with high-voltage systems. Direct contact to the ESI emitter assembly can result in injury or death. Experimental precautions include shielding, insulting, and limiting the exposure of electrical components. Visual signs indicating high voltage should be displayed, and foot traffic within the surrounding area is limited during experiments. The high voltage should be turned off during removal and placement of samples.

3. The mid-IR laser source is a Class IV laser system, thus precautionary measures must be taken to prevent injury or death. Appropriately rated laser safety goggles and clothing must be worn to avoid laser beam exposure. Beam blocks and enclosure tubes should be used to shield the laser beam throughout the optical path. Proper protection should also be used for the Class II laser alignment diode (635 nm wavelength).
4. Helium, argon, and carbon dioxide can also be used as alternative drift gases and will result in different CCS values.
5. To reduce any environmental shock to the cells, avoid washing with water and store the adherent cells in the incubator between analyses. Analysis should be performed within a couple of minutes of washing the cells with 10× diluted PBS.

---

## Acknowledgments

We thank Lida Parvin for providing a cell stock of SK-N-AS. Research was sponsored by the U.S. Army Research Office and the Defense Advanced Research Projects Agency and was accomplished under Cooperative Agreement Number W911NF-14-2-0020. The views and conclusions contained in this document are those of the authors and should not be interpreted as representing the official policies, either expressed or implied, of the Army Research Office, DARPA, or the U.S. Government.

## References

1. Dunn WB, Bailey NJC, Johnson HE (2005) Measuring the metabolome: current analytical technologies. *Analyst* 130(5):606–625. <https://doi.org/10.1039/b418288j>
2. Park JO, Rubin SA, Xu YF, Amador-Noguez D, Fan J, Shlomi T, Rabinowitz JD (2016) Metabolite concentrations, fluxes and free energies imply efficient enzyme usage. *Nat Chem Biol* 12(7):482–489. <https://doi.org/10.1038/nchembio.2077>
3. Cooks RG, Ouyang Z, Takats Z, Wiseman JM (2006) Ambient mass spectrometry. *Science* 311(5767):1566–1570. <https://doi.org/10.1126/science.1119426>
4. Wu CP, Dill AL, Eberlin LS, Cooks RG, Ifa DR (2013) Mass spectrometry imaging under ambient conditions. *Mass Spectrom Rev* 32(3):218–243. <https://doi.org/10.1002/mas.21360>
5. Chiang S, Zhang WP, Ouyang Z (2018) Paper spray ionization mass spectrometry: recent advances and clinical applications. *Expert Rev Proteomics* 15(10):781–789. <https://doi.org/10.1080/14789450.2018.1525295>
6. Pavlovich MJ, Musselman B, Hall AB (2018) Direct analysis in real time mass spectrometry (DART-MS) in forensic and security applications. *Mass Spectrom Rev* 37(2):171–187. <https://doi.org/10.1002/mas.21509>
7. Alford A (1975) Environmental applications of mass spectrometry. *Biomed Mass Spectrom* 2(5):229–253. <https://doi.org/10.1002/bms.1200020502>
8. Ifa DR, Eberlin LS (2016) Ambient ionization mass spectrometry for cancer diagnosis and surgical margin evaluation. *Clin Chem* 62(1):111–123. <https://doi.org/10.1373/clinchem.2014.237172>
9. Li H, Balan P, Vertes A (2016) Molecular imaging of growth, metabolism, and antibiotic inhibition in bacterial colonies by laser ablation electrospray ionization mass spectrometry. *Angew Chem Int Ed* 55(48):15035–15039. <https://doi.org/10.1002/anie.201607751>

10. Muller T, Oradu S, Ifa DR, Cooks RG, Krautler B (2011) Direct plant tissue analysis and imprint imaging by desorption electrospray ionization mass spectrometry. *Anal Chem* 83 (14):5754–5761. <https://doi.org/10.1021/ac201123t>
11. Gross JH (2014) Direct analysis in real time—a critical review on DART-MS. *Anal Bioanal Chem* 406(1):63–80. <https://doi.org/10.1007/s00216-013-7316-0>
12. Nemes P, Vertes A (2007) Laser ablation electrospray ionization for atmospheric pressure, in vivo, and imaging mass spectrometry. *Anal Chem* 79(21):8098–8106. <https://doi.org/10.1021/ac071181r>
13. Shrestha B, Vertes A (2014) High-throughput cell and tissue analysis with enhanced molecular coverage by laser ablation electrospray ionization mass spectrometry using ion mobility separation. *Anal Chem* 86(9):4308–4315. <https://doi.org/10.1021/ac500007t>
14. Gaye MM, Kurulugama R, Clemmer DE (2015) Investigating carbohydrate isomers by IMS-CID-IMS-MS: precursor and fragment ion cross-sections. *Analyst* 14(20):6922–6932. <https://doi.org/10.1039/c5an00840a>
15. Paglia G, Kliman M, Claude E, Geromanos S, Astarita G (2015) Applications of ion-mobility mass spectrometry for lipid analysis. *Anal Bioanal Chem* 407(17):4995–5007. <https://doi.org/10.1007/s00216-015-8664-8>
16. Chouinard CD, Wei MS, Beekman CR, Kemperman RHJ, Yost RA (2016) Ion mobility in clinical analysis: current progress and future perspectives. *Clin Chem* 62(1):124–133. <https://doi.org/10.1373/clinchem.2015.238840>
17. Kliman M, May JC, McLean JA (2011) Lipid analysis and lipidomics by structurally selective ion mobility-mass spectrometry. *Biochim Biophys Acta* 1811(11):935–945. <https://doi.org/10.1016/j.bbaliip.2011.05.016>
18. Kanu AB, Dwivedi P, Tam M, Matz L, Hill HH (2008) Ion mobility-mass spectrometry. *J Mass Spectrom* 43(1):1–22. <https://doi.org/10.1002/jms.1383>
19. Stopka SA, Mansour TR, Shrestha B, Marechal E, Falconet D, Vertes A (2016) Turnover rates in microorganisms by laser ablation electrospray ionization mass spectrometry and pulse-chase analysis. *Anal Chim Acta* 902:1–7. <https://doi.org/10.1016/j.aca.2015.08.047>
20. Stopka S, Agtuca B, Khattar R, Anderton C, Koppelaar D, Pasa-Tolic L, Stacey G, Vertes A (2017) Metabolomics of biological nitrogen fixation explored by laser ablation electrospray ionization mass spectrometry combined with fluorescence microscopy. Abstracts of Papers of the American Chemical Society 254
21. De Clercq E (2005) Recent highlights in the development of new antiviral drugs. *Curr Opin Microbiol* 8(5):552–560. <https://doi.org/10.1016/j.mib.2005.08.010>
22. Otterbein LE, Bach FH, Alam J, Soares M, Lu HT, Wysk M, Davis RJ, Flavell RA, Choi AMK (2000) Carbon monoxide has anti-inflammatory effects involving the mitogen-activated protein kinase pathway. *Nat Med* 6 (4):422–428
23. Jacobson RS, Thurston RL, Shrestha B, Vertes A (2015) In situ analysis of small populations of adherent mammalian cells using laser ablation electrospray ionization mass spectrometry in transmission geometry. *Anal Chem* 87 (24):12130–12136. <https://doi.org/10.1021/acs.analchem.5b02971>